

## Article

# Improvement of Climate Resource Utilization Efficiency to Enhance Maize Yield through Adjusting Planting Density

Wenming Wu <sup>1</sup>, Lin Zhang <sup>1</sup>, Zhaokang Chu <sup>2</sup>, Wei Yue <sup>3</sup>, Ying Xu <sup>3</sup>, Chen Peng <sup>1</sup>, Xiang Chen <sup>2</sup>, Lili Jing <sup>1</sup>, Wei Ma <sup>4,\*</sup> and Shiji Wang <sup>1,\*</sup>

<sup>1</sup> Maize Research Center, Anhui Academy of Agricultural Sciences, Hefei 230001, China

<sup>2</sup> School of Agronomy, Anhui Agricultural University, Hefei 230036, China

<sup>3</sup> Agricultural Meteorological Center of Anhui Province, Hefei 230031, China

<sup>4</sup> Institute of Crop Sciences, Chinese Academy of Agricultural Sciences, Beijing 100081, China

\* Correspondence: mawei@cass.cn (W.M.); wangshijiy@163.com (S.W.)

**Abstract:** The sustainable high yield of crops is critically important under the current situation of global climate warming. In order to improve regional yield, it is urgent to clarify the limiting factors of local grain yield and change the traditional planting measurements to adapt to the warming climate and make full use of climate resources. Long-term field experiments over seven years from 2014 to 2021 were conducted with the same maize cultivar (i.e., Luyu9105) with seven planting density treatments:  $3.0 \times 10^4$  (D1),  $4.5 \times 10^4$  (D2),  $6.0 \times 10^4$  (D3),  $7.5 \times 10^4$  (D4),  $9.0 \times 10^4$  (D5),  $10.5 \times 10^4$  (D6), and  $12.0 \times 10^4$  (D7) plants per hectare in Taihe and Hefei, which belong to the southern Huang-Huai-Hai (SHHH) and southeast (SE) maize-producing areas in China. According to the field experiment data, differences in grain yield, ear number, kernel number per spike, and 1000-kernel weight of different treatments were analyzed. The utilization efficiency of climate resources in Taihe and Hefei was calculated using daily solar radiation, mean temperature, and precipitation data. The results showed that Taihe had 7.8% higher solar radiation during the growing season of maize than Hefei, while accumulated temperature  $\geq 10$  °C ( $AT_{10}$ ) was 3.9% lower than Hefei. The grain yields of different planting densities in Taihe were 9.7–23.6% higher than in Hefei. The agronomic optimal planting density (AOPD) was  $8.6 \times 10^4$  plants  $ha^{-1}$  in Taihe and  $8.0 \times 10^4$  plants  $ha^{-1}$  in Hefei. Compared to the actual grain yields, when the agronomic optimal planting densities were adopted, the simulated yield increased by 51.3% and 59.6%, respectively. The radiation utilization efficiency, temperature utilization efficiency, and precipitation utilization efficiency in Taihe were 12.9%, 24.6%, and 26.7% higher than the values of Hefei, respectively, and D4 and D5 treatments had significantly higher climatic resource utilization efficiency than D1 and D2 treatment. The grain yield was negatively correlated with accumulated temperature  $\geq 10$  °C and positively correlated with solar radiation. The multiple linear regression model among solar radiation, accumulated temperature was  $\geq 10$  °C, and grain yield was  $y = 0.550R - 0.562AT_{10} + 14,593.6$  ( $R = 0.379$ ). Accumulated temperature  $\geq 10$  °C was the main climatic factor affecting the grain yield due to the higher occurrence probability of a maximum temperature  $\geq 35$  °C. Overall, in the future, increasing planting density and alleviating heat stress may enhance grain yield. These results could provide cultivation measurements with regional characteristics to adapt to the local climate and maximize the utilization efficiency of climatic resources.



**Citation:** Wu, W.; Zhang, L.; Chu, Z.; Yue, W.; Xu, Y.; Peng, C.; Chen, X.; Jing, L.; Ma, W.; Wang, S. Improvement of Climate Resource Utilization Efficiency to Enhance Maize Yield through Adjusting Planting Density. *Agronomy* **2023**, *13*, 846. <https://doi.org/10.3390/agronomy13030846>

Academic Editor: Rosa Porcel

Received: 23 February 2023

Revised: 7 March 2023

Accepted: 8 March 2023

Published: 14 March 2023



**Copyright:** © 2023 by the authors. Licensee MDPI, Basel, Switzerland. This article is an open access article distributed under the terms and conditions of the Creative Commons Attribution (CC BY) license (<https://creativecommons.org/licenses/by/4.0/>).

**Keywords:** maize; grain yield; planting density; solar utilization efficiency; temperature utilization efficiency; precipitation utilization efficiency

## 1. Introduction

As the population of the world increases, it is necessary to increase the global crop yield to mitigate food shortages and guarantee food security [1]. However, as the global climate warms, extreme climate events, i.e., drought, heat damage, and wind, have increased across

many of the world's regions and pose new challenges to food security [2,3]. The southern Huang-Huai-Hai (SHHH) maize region and hilly maize area in the southeast (SE) are the southernmost regions of China's main maize production areas. Due to their particular geographical locations, the climatic conditions differ from other maize regions, i.e., the northeast and northwest maize regions, especially under the background of global climate warming. Thus, in order to make full use of climate resources, alleviate the negative effects of climate warming, and improve the local grain yield, it is necessary to clarify the impacted factors of maize production in these two regions and change the ordinary cultivation methods to adapt to global climate change, which is helpful for local maize cultivation.

Grain yield is interactively determined by the genetic factors of the variety itself [4], climatic factors (i.e., solar radiation, temperature, and precipitation) [5,6], and agronomic measures (i.e., planting density, planting date, row space, and fertilization strategy) [7–9]. Breeding accounts for 50% of the grain yield [4]. Previous research has demonstrated that maize yield potential has not undergone genetic improvement in hybrid ears, yet high population density tolerance has undergone substantial genetic improvement [10]. Changing the planting density results in a high grain yield via prolongation of the functional leaf period of maize leaves and significantly increases the leaf area index [1,11], which can make full use of available climate and nitrogen resources [12,13]. However, the effects of planting density on the grain yield depend on the compound interaction of hybrid, climatic factors, and other managements, i.e., soil fertility, planting date, and row spacing management [14,15]. Yield does not always increase with the increase in the planting density of different regions, especially with global warming [16,17]. Therefore, under such conditions, it is vital to elucidate the optimal planting density of different regions.

Adjusting the planting density is an effective measure for improving grain yield, which can change the distribution and utilization of light, temperature, and other climatic factors [18,19]. Solar radiation, heat resources, and water are the most important factors that affect maize growth and development [20–22], especially solar radiation [23,24]. However, as it has been influenced by global climate change and environmental pollution, a slightly decreasing trend of solar radiation in China has reduced dry matter weight by 12.3 kg ha<sup>-1</sup> per year [25–27], and other results also indicated that a 100 MJ decrease in accumulated photosynthetically active radiation resulted in an 850 kg ha<sup>-1</sup> reduction in maize grain yield in China [28]. Insufficient solar radiation will detrimentally affect photosynthetic efficiency and may induce the occurrence of barren stalks and stalk lodging [5]. Additionally, the Global Climate Model projected that the mean maximum (minimum) temperature during the growing season of maize would increase by 1.9 °C and 3.7 °C (1.5 °C and 3.2 °C) in the 2040s and 2080s, respectively [29]. As the climate has changed, the growing degree days have increased in northeast China, which may accelerate maize growth development [15,26] and decrease grain yield [30].

Numerous studies have analyzed the relationship between climatic factors and grain yield among different cultivated regions [31,32]. Therefore, identifying grain yield and its driving factors is vital to ensure sustainable grain production. In northwestern China, grain yield was positively affected by solar radiation and thermal time during the growth stage, and regional solar radiation had a greater impact on the grain yield than thermal time in northwestern China, northeastern China, and northern China [23]. Conversely, Zhang reported that a negative impact of temperature was found in northeastern China and the Northern China Plain, which may be due to the fact that the temperature had exceeded the 32 °C threshold of maize growth [26].

However, existing studies have mainly focused on the northern China area, so little is known about the maize development in SHHH and SE, the difference between the two regions, and the relationship between grain yield and climatic resources. Our study could clarify the optimal planting density in the two regions, the yield difference, and the causes leading to this difference, which could provide guidance for research in other areas of the world. In this context, we selected two sites, Taihe (33°25' N, 115°60' E) and Hefei (31°57' N, 117°11' E), which are located in the SHHH and SE areas, respectively. Long-term

field experiments were conducted with the same maize cultivar (i.e., Luyu9105), the same planting density treatments, and other management measures over seven years. The goals of this study were as follows: (1) to determine the optimal planting density in these two regions; (2) to clarify the yield differences between two maize-producing areas and explore the limiting factors of regional maize production; (3) to quantify the relationship between solar radiation, heat resources, and grain yield.

## 2. Materials and Methods

### 2.1. Experimental Site

The field experiments were carried out in Taihe (33°25' N, 115°60' E) during 2014–2021 and Hefei during 2014–2017 (31°57' N, 117°11' E), which are two summer-sown maize areas in SHHH and SE, respectively. The cropping pattern of these two regions is largely a winter wheat–summer maize double-cropping system, with shallow rotary tillage for winter wheat and no tillage for summer maize. The soil types in Taihe and Hefei are lime concretion black soil and yellow cinnamon soil, respectively. The physical and chemical characteristics of the topsoil (0–20 cm) during experiments are shown in Table 1.

**Table 1.** The physical and chemical characteristics of the topsoil during the experiment at Taihe and Hefei.

Sites	Years	pH	Soil Organic Carbon (g kg <sup>-1</sup> )	Alkali-Hydrolyzable N (mg kg <sup>-1</sup> )	Available P (mg kg <sup>-1</sup> )	Available K (mg kg <sup>-1</sup> )
Taihe	2014	7.2	22.1	120.6	43.1	227.9
	2015	6.9	21.7	133.1	38.1	271.2
	2016	7.2	22.3	169.7	40.5	249.7
	2017	7.1	22.1	159.8	35.9	187.6
	2018	6.9	20.6	146.2	30.8	186.4
	2020	6.9	22.8	175.6	39.1	201.0
	2021	6.8	20.6	145.9	38.6	156.7
Hefei	2014	6.9	21.6	118.4	25.4	269.6
	2015	6.5	19.8	129.8	26.5	224.9
	2016	6.7	20.6	156.4	21.1	200.7
	2017	6.7	19.1	127.1	18.6	235.8

The daily mean temperature ( $T_{mean}$ ) and precipitation (Prec.) were obtained from the National Meteorological Data Center (<http://data.cma.cn/>). The meteorological data details of Taihe and Hefei are shown in Table 2.

**Table 2.** The meteorological data details at Taihe and Hefei.

	Taihe 2012–2021	Hefei 2012–2021	Taihe 2014–2021	Hefei 2014–2017
The annual mean temperature (°C)	15.7	16.2	–	–
The mean annual total precipitation (mm)	1000	1033	–	–
The mean temperature from June to October (°C)	–	–	23.7	24.6
The mean total precipitation from June to October (mm)	–	–	657	745.3

Note: – means there were no data.

### 2.2. Experimental Design

Fully randomized complete blocks with three replications were designed at two experimental sites, respectively, by using the same cultivar, Luyu 9105, as it is widely grown in these two experimental sites and is high-yielding, resistant to multiple leaf diseases, i.e., bipolarismaydis and rust disease, and highly adaptable. Seven different

planting densities were designed, which were  $3.0 \times 10^4$  (D1),  $4.5 \times 10^4$  (D2),  $6 \times 10^4$  (D3),  $7.5 \times 10^4$  (D4),  $9 \times 10^4$  (D5),  $10.5 \times 10^4$  (D6), and  $12.0 \times 10^4$  (D7) plants  $\text{ha}^{-1}$ . D1 was not designed from 2017 to 2021. The size of each plot was  $24.12 \text{ m}^2$  (6.7 m length  $\times$  3.6 m width), with six rows.

The maize was sown with a row spacing of 60 cm and a depth of 5 cm of the seeds. The details of the planting dates and harvesting dates in the two sites are shown in Table 3. The application rate of pure N, phosphorus, and potassium fertilizer in experimental sites were  $240 \text{ kg ha}^{-1}$ ,  $105 \text{ kg ha}^{-1}$ , and  $135 \text{ kg ha}^{-1}$  using urea (containing N 46%) and compound fertilizer (containing N,  $\text{P}_2\text{O}_5$ ,  $\text{K}_2\text{O}$  15:15:15); for the insufficient potassium fertilizer, we applied  $\text{K}_2\text{SO}_4$  (containing  $\text{K}_2\text{O}$  50%) as a supplement. All of the fertilizer was applied to each plot prior to sowing. According to the actual situation in the field, the recommended dosages of chemical agents were used to control diseases, pests, and weeds.

**Table 3.** The planting dates and harvesting dates in Taihe and Hefei.

Years	Planting Date (Month/Day)		Harvesting Date (Month/Day)	
	Taihe	Hefei	Taihe	Hefei
2014	6/17	6/21	10/03	10/14
2015	6/17	6/21	10/03	10/14
2016	6/13	6/28	10/06	10/18
2017	6/12	6/15	10/13	10/10
2018	6/05	–	9/27	–
2019	–	–	–	–
2020	6/05	–	9/27	–
2021	6/05	–	9/27	–

Note: – means experiment was not carried out in this year.

### 2.3. Research Methods

#### 2.3.1. Grain Yield

At the maturity stage, 30 ears were selected for harvest in the middle three rows of each plot to determine the yield and its components, i.e., the row number, kernel number per ear, and 1000-kernel weight. A total of 100 kernels were sampled in the middle of each ear and weighed, then multiplied by 10 to determine the 1000-kernel weight. All the kernels were air-dried and the grain moisture content was determined using a grain moisture tester (PM-8188-A). The grain yield was calculated at 14% moisture, which is the standard for maize storage or sale in China (GB/T29890-2013). The grain yield was calculated as follows [33,34]:

$$y \text{ (kg ha}^{-1}\text{)} = \frac{A \times B \times C \times (1 - D)}{10^6 \times (1 - 14\%)} \quad (1)$$

where  $y$  is the grain yield,  $A$  is the harvested ears ( $\text{ears ha}^{-1}$ ),  $B$  is the kernel number per ear,  $C$  is the 1000-kernel weight ( $\text{g } 1000 \text{ kernels}^{-1}$ ), and  $D$  is the sample moisture content (%).

#### 2.3.2. Dry Matter Accumulation and Dry Matter Translocation (DMA and DMT)

At the silking and maturity stage, three adjacent plants were sampled with three replicates. Fresh samples were heated at  $105 \text{ }^\circ\text{C}$  in an oven for half an hour to inactivate the enzymes and then dried at  $80 \text{ }^\circ\text{C}$  to a constant weight to determine their DMA. The DMT from the vegetative organs to the grain between silking and maturity, the DMA at the post-silking stage, and the contribution of dry matter at the post-silking stage to the grain weight (CDMGW) were calculated following the methods of Wu et al. [34].

$$\text{DMT} = \text{DMA at the silking stage} - \text{DMA at the maturity stage} \quad (2)$$

$$\text{The DMA at the post-silking stage} = \text{Grain weight at maturity stage} - \text{DMT} \quad (3)$$

$$\text{Contribution of DMT before the silking stage to grain yield (\%)} = \frac{\text{DMT}}{\text{Grain yield}} \times 100 \quad (4)$$

$$\text{CDMGW(\%)} = \frac{\text{DMA at the post-silking stage}}{\text{Grain yield}} \times 100 \quad (5)$$

### 2.3.3. Climatic Data

Daily weather records during the growing season from 2014 to 2021, including daily mean temperature ( $T_{mean}$ ), maximum temperature ( $T_{max}$ ), precipitation (Prec.), and sunshine hours (SH), were obtained from the National Meteorological Data Center (<http://data.cma.cn/>).

### 2.3.4. Accumulated Temperature $\geq 10$ °C ( $AT_{10}$ )

$AT_{10}$  was calculated by summing the daily mean temperatures during the growing season when the daily temperature was above 10 °C. The equation is as follows:

$$AT_a = \sum_0^n (T_{mean} - 10) \quad (6)$$

### 2.3.5. Solar Radiation

The total solar radiation model constructed based on the measured data in this study requires astronomical radiation or clear sky radiation. Therefore, the radiation formula in the Penman–Monteith model recommended by FAO56 was used to calculate these two elements. Based on the solar radiation data and sunshine hour data of radiation stations in the Huaihe River Basin from 1961 to 2010, with the percentage of sunshine as the independent variable, the multiple regression analysis method was used to fit the empirical coefficient a and b values, which revised the recommended values of FAO56. For the solar radiation estimation model, see the following formulas:

$$R_0 = G_{sc} d_r (\omega_s \sin \varphi \sin \delta + \cos \varphi \cos \delta \sin \omega_s) / \pi \quad (7)$$

$$d_r = 1 + 0.033 \cos \left( \frac{2\pi}{365} J \right) \quad (8)$$

$$\delta = 0.409 \sin \left( \frac{2\pi}{365} J - 1.39 \right) \quad (9)$$

$$\omega_s = \arccos(-\tan \varphi \tan \delta) \quad (10)$$

$$R_s = R_0 (0.172 + 0.521n/N) \quad (11)$$

$$N = \frac{24}{\pi} \omega_s \quad (12)$$

where  $R_0$  is the astronomical radiation,  $R_s$  is the clear sky radiation,  $G_{sc}$  is the solar constant (118.109 MJ/(m<sup>2</sup>·d)),  $d_r$  is the “Sun–Earth distance” correction factor,  $\delta$  is the solar declination,  $\varphi$  is the geographical latitude,  $\omega_s$  is the hour angle at sunset, and  $\pi$  is 3.1415926,  $n$  is the actual sunshine hour duration (unit h),  $N$  is the maximum possible sunshine hour duration (unit h), and  $n/N$  is the relative sunshine hours.

### 2.3.6. Utilization Efficiency of Solar Radiation, Temperature, and Precipitation

The formulas for the calculation of solar radiation utilization efficiency ( $RUE$ ) and temperature utilization efficiency ( $TUE$ ) are as follows [35]:

$$RUE = \frac{q \times y}{\sum R_s} \times 100\% \quad (13)$$

where  $y$  is the average grain yield of each experimental site and  $q$  is the conversion coefficient of dry matter to heat energy, and the value is  $0.0175 \text{ MJ g}^{-1}$ .  $\sum R_s$  is the total solar radiation during the maize growing season ( $\text{MJ m}^{-2}$ ).

$$TUE = \frac{Y}{\sum AT_a} \quad (14)$$

$TUE$  uses the units  $\text{g, m}^{-2}$  and  $^{\circ}\text{C}^{-1}$ .  $\sum AT_a$  is the accumulated temperature  $\geq 10^{\circ}\text{C}$  during the maize growing season ( $^{\circ}\text{C d}$ ).

$$PUE = \frac{Y}{\sum P} \quad (15)$$

$PUE$  is the precipitation utilization efficiency with the units  $\text{g}$  and  $\text{mm}^{-1}$ .  $\sum P$  is the total precipitation during the maize growing season ( $\text{mm}$ ).

### 2.3.7. Statistical Analysis

Treatments' effects on the grain yield and its components and utilization efficiency of climate resources were analyzed using analysis of variance (ANOVA) at the 5% significance level in SPSS 13.0 (SPSS, Chicago, IL, USA). Significant differences among means were determined by least-significant-difference (LSD) multiple-range tests at the 5% level.

The regression and stepwise multiple regression were analyzed to test the relationship between grain yield and grain components with meteorological data using SPSS 13.0 (SPSS, Chicago, IL, USA). The other data were analyzed using Excel 2016 (Redmond, WA, USA). All of the figures were drawn using SigmaPlot 10.0 (Systat, San Jose, CA, USA) and Excel 2016.

## 3. Results

### 3.1. Differences in Yield and Its Components

Yield was significantly affected by planting density, year, and experimental site (Table 4). The interaction values of planting density  $\times$  year, planting density  $\times$  site, year  $\times$  site, and planting density  $\times$  year  $\times$  site were significant. A similar result was also observed for kernel number per ear, whereas ear number was only significantly different between different planting densities. As for 1000-kernel weight, the planting density  $\times$  site interaction and the year  $\times$  site interaction were not significant.

**Table 4.** Analysis of variance for grain yield and its components.

Factor	Yield	1000-Kernel Weight	Kernel Number	Ear Number
Density (D)	172.3 **	47.1 **	178.4 **	9.9 **
Year (Y)	97.5 **	89.1 **	99.1 **	1.2
Site (S)	446.3 **	125.2 **	370.2 **	0.009
D $\times$ Y	6.8 **	4.4	12.5 **	1.1
D $\times$ S	5.6 **	1.0	8.5 **	0.01
Y $\times$ S	53.6 **	70.5 **	17.0 **	0.07
D $\times$ S $\times$ Y	3.0 **	2.0 *	3.4 **	0.02

Note: \*\* indicates there was a significant difference at 1% level; \* indicates there was a significant difference at 5% level.

Box plots for the yield, kernel number per ear, and 1000-kernel weight of maize in Taihe and Hefei are shown in Figure 1. The average grain yields of different planting densities from D1 to D7 in Taihe were  $6155.4 \text{ kg ha}^{-1}$ ,  $8385.3 \text{ kg ha}^{-1}$ ,  $10,260.3 \text{ kg ha}^{-1}$ ,  $10,905.1 \text{ kg ha}^{-1}$ ,  $10,938.1 \text{ kg ha}^{-1}$ ,  $9921.1 \text{ kg ha}^{-1}$ , and  $9753.4 \text{ kg ha}^{-1}$ , respectively. Grain yield increased as planting density increased from D1 to D5 and then decreased from D5 to D7. Ear number per hectare increased, whereas 1000-kernel weight and kernel number per ear decreased as planting density increased. The average grain yields in Hefei were  $5557.5 \text{ kg ha}^{-1}$ ,  $7160.1 \text{ kg ha}^{-1}$ ,  $8479.2 \text{ kg ha}^{-1}$ ,  $9041.1 \text{ kg ha}^{-1}$ ,  $8718.9 \text{ kg ha}^{-1}$ ,

8563.7 kg ha<sup>-1</sup>, and 8213.0 kg ha<sup>-1</sup> from D1 to D7. Grain yield increased as planting density increased from D1 to D4 and then decreased from D4 to D7. Taihe produced a significantly higher maize yield overall, and the values for different planting densities were 9.7%, 17.7%, 20.7%, 21.3%, 23.6%, 16.3%, and 21.3% higher than that in Hefei, respectively.

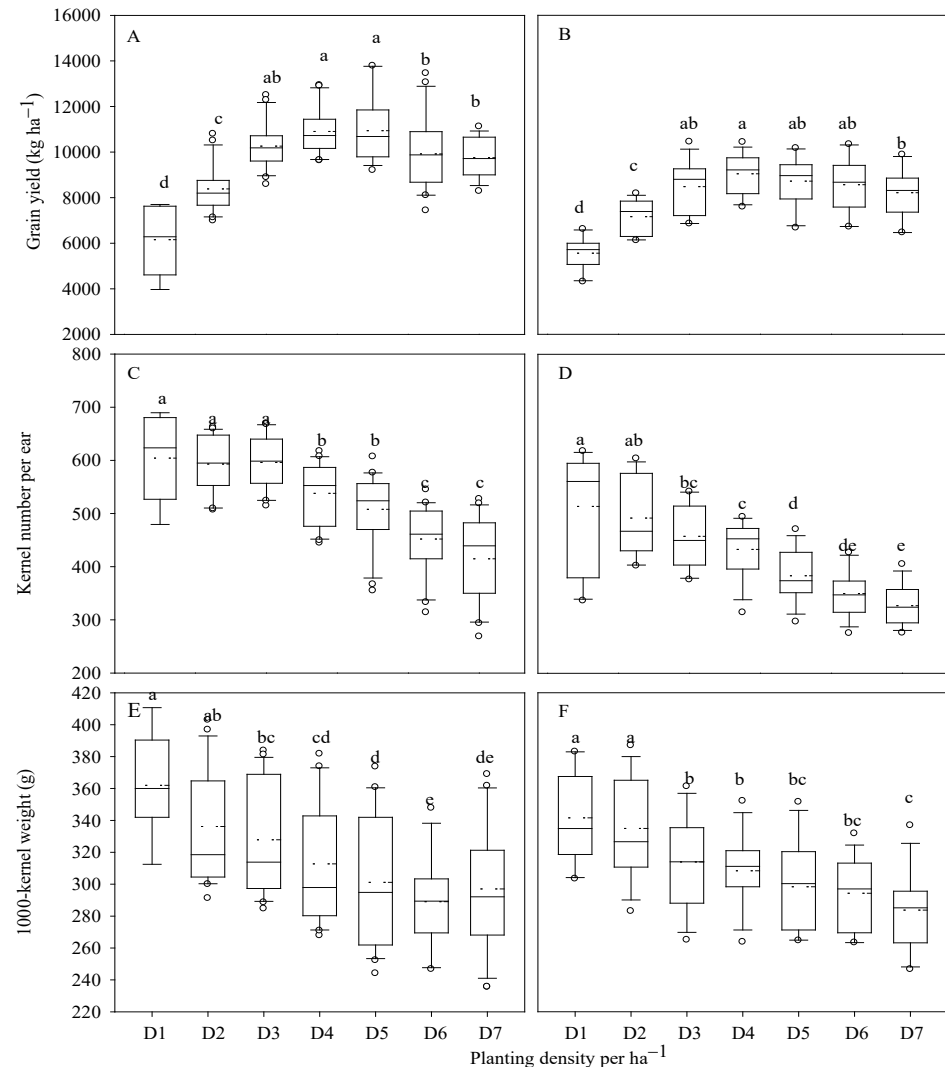


**Figure 1.** Grain yield and its components under different planting densities in different sites. Note: Figure (A,C,E) represent grain yield, kernel number per ear, and 1000-kernel weight in Taihe. Figure (B,D,F) represent grain yield, kernel number per ear, and 1000-kernel weight in Hefei. Different letters above the boxes indicate significant differences between different planting densities.

### 3.2. Regression of Grain Yield and Its Components

The regression models between grain yield and its components are shown in Figure 2. A positive relationship between grain yield and ear number was found in Taihe and Hefei (Figure 2C,F), but there was no significant relationship between grain yield and kernel number per ear or 1000-kernel weight (Figure 2A,B,D,E) when combining the data of Taihe and Hefei, there was a positive relationship between grain yield and both ear number and kernel number per ear (Figure 2H,I). In conclusion, the grain yield was positively correlated with the ear number; the main difference in yields between Taihe and Hefei may be due to the kernel numbers per ear.

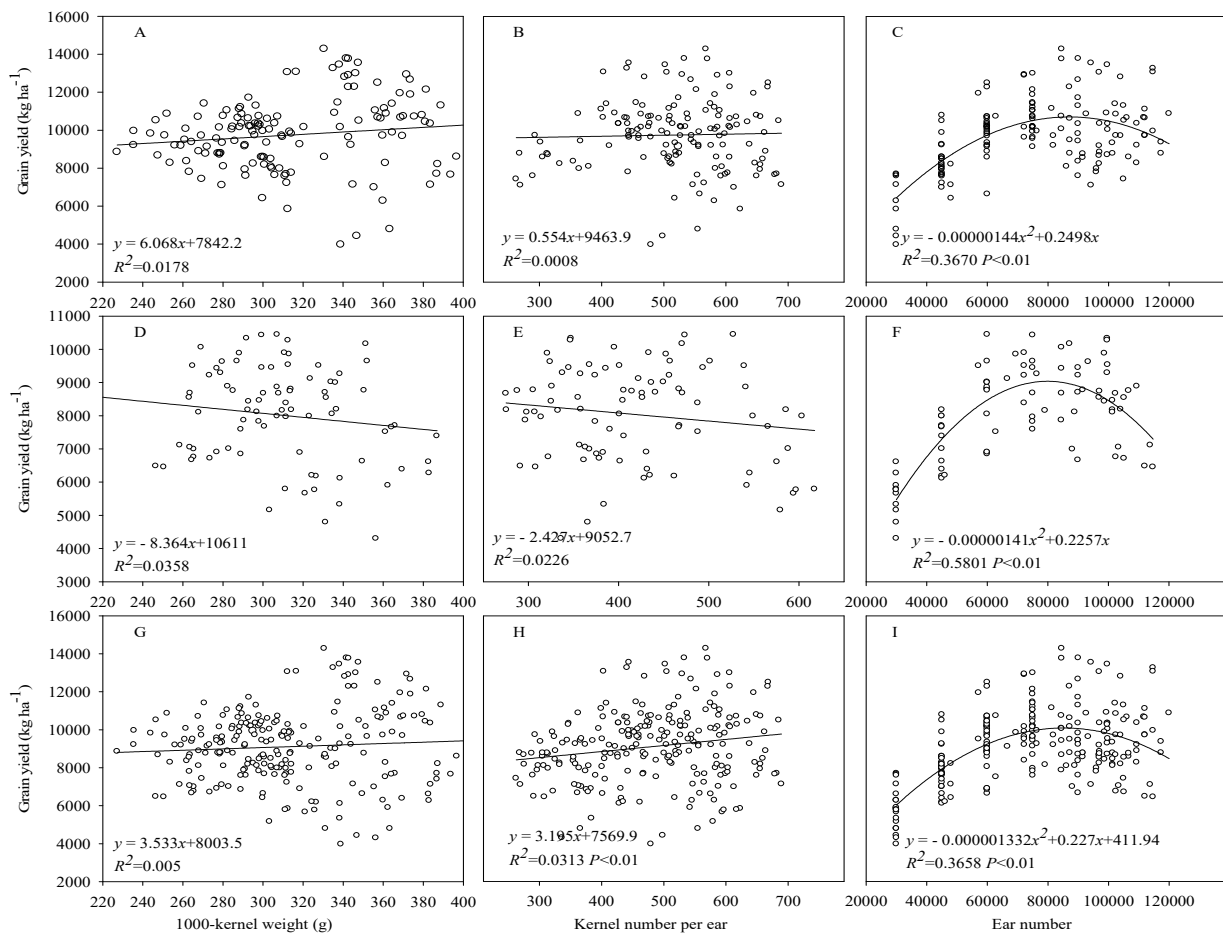


**Figure 2.** Relationship between grain yield and its components. Note: Figure (A–C) represent the relationship between grain yield and yield components in Taihe. Figure (D–F) represent the relationship between grain yield and yield components in Hefei. Figure (G–I) represent the relationship between grain yield and yield components in Taihe and Hefei.

The quadratic model observed that, between grain yield and planting density (Table 5), with the significant regression equation  $y = -1.44 \times 10^{-6}x^2 + 0.2498x$  ( $R^2 = 0.367$ ) in Taihe, the agronomic optimal planting density (AOPD) was  $8.6 \times 10^4$  plants  $ha^{-1}$  based on the equation, and yield at the AOPD was 10,768.3  $kg\ ha^{-1}$  (Table 5). The 95% CI broadened from  $7.6\sim 9.7 \times 10^4$  plants  $ha^{-1}$  between the lower and upper limit in Taihe. The significant regression equation in Hefei was  $y = -1.41 \times 10^{-6}x^2 + 0.2257x$  ( $R^2 = 0.5801$ ). The AOPD was  $8.0 \times 10^4$  plants  $ha^{-1}$ , and the yield at the AOPD was 9025.6  $kg\ ha^{-1}$ . The 95% CI broadened from  $6.9\sim 9.0 \times 10^4$  plants  $ha^{-1}$  between the lower and upper limit in Hefei. Correspondingly, these results suggested that the simulated grain yield in Taihe was 19.3% higher than in Hefei.

**Table 5.** Quadratic equations that best fit the yield–density relations, agronomic optimal planting density (AOPD), 95% confidence interval (CI) of the AOPD, yield at the AOPD, and at the upper and lower limits of AOPD.

Site	Equation	R <sup>2</sup>	Planting Density 95% CI			Yield 95% CI		
			AOPD	Lower 10 <sup>4</sup> Plants ha <sup>-1</sup>	Upper	AOPD	Lower kg ha <sup>-1</sup>	Upper
Taihe	$y = -1.44 \times 10^{-6}x^2 + 0.2498x$	0.3670	8.6	7.6	9.7	10,768.3	10,610.8	10,610.8
Hefei	$y = -1.41 \times 10^{-6}x^2 + 0.2257x$	0.5801	8.0	6.9	9.0	9025.6	8870.1	8870.1

### 3.3. Difference in DMA and DMT

The aboveground dry matter accumulation of different sites and different planting densities are shown in Figure 3. The DMA weight after the silking stage in Taihe accounted for 54.1~62.9% in 2017 and 55.2~69.6% in 2018; the values in Hefei were 54.3~63.5% in 2016 and 50.0~59.0% in 2018. There was a significant difference in the DMA of different sites and planting densities. Taihe had a higher DMA than Hefei. As planting density increased, the DMA increased. However, D4 and D5 treatments decreased the DMT and the contribution of DMT before the silking stage to the grain stage and enhanced the contribution of dry matter at the post-silking stage to the grain weight more than other treatments (Table 6).

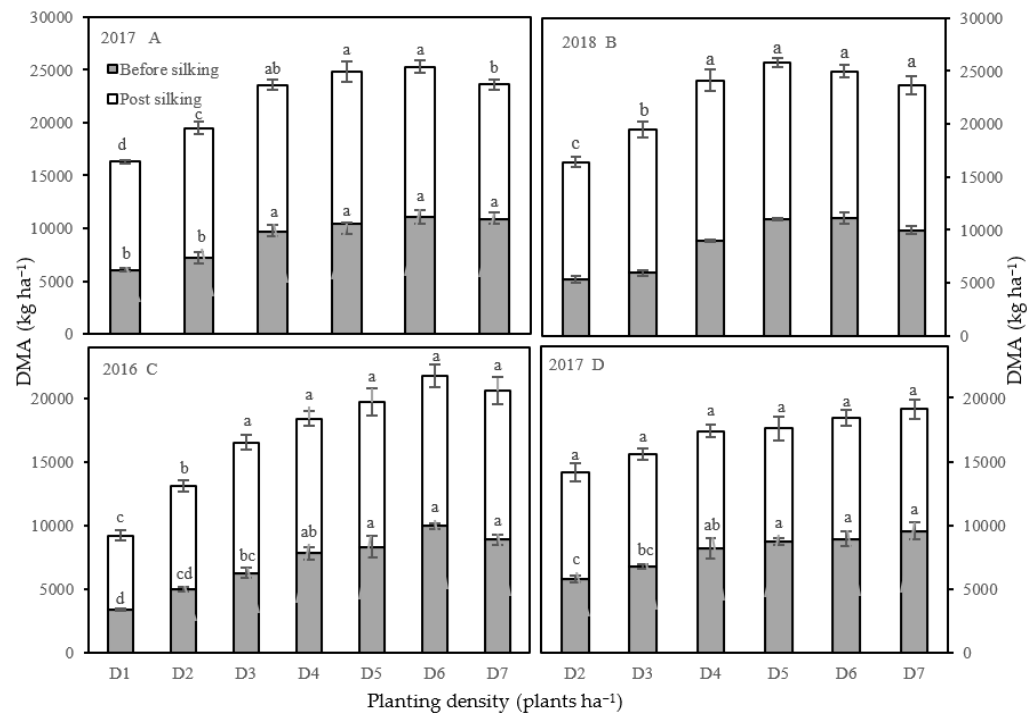


**Figure 3.** Aboveground DMA of different sites and planting densities. Note: Figure (A,B) represent DMA in Taihe. Figure (C,D) represent DMA in Hefei. Different letters above the bars indicate significant differences between different planting densities.

**Table 6.** DMT from vegetative organs to grain and accumulation amount at the post-silking stage.

Site	Year	Treatment	DMT before the Silking Stage (kg ha <sup>-1</sup> )	Contribution of DMT before the Silking Stage to Grain (%)	DMA at the Post-Silking Stage (kg ha <sup>-1</sup> )	CDMGW (%)
Taihe	2017	D2	1932.1	23.3	6360.2	76.7
		D3	1918.2	18.6	8412.6	81.4
		D4	1808.4	15.0	10,245.9	85.0
		D5	2884.4	25.1	8595.2	74.9
		D6	3418.1	31.5	7424.2	68.5
		D7	3423.7	36.7	5916.2	63.3
		2018	D2	2858.0	34.6	5392.4
	D3		3554.5	35.5	6467.7	64.5
	D4		2053.2	15.7	11,052.3	84.3
	D5		1707.4	13.1	11,343.0	86.9
	D6		3760.0	37.2	6335.8	62.8
	D7		3768.9	38.0	6159.0	62.0

Table 6. Cont.

Site	Year	Treatment	DMT before the Silking Stage (kg ha <sup>-1</sup> )	Contribution of DMT before the Silking Stage to Grain (%)	DMA at the Post-Silking Stage (kg ha <sup>-1</sup> )	CDMGW (%)
Hefei	2016	D1	1029.9	21.4	3777.6	78.6
		D2	1420.6	21.1	5311.5	78.9
		D3	1832.6	21.8	6592.1	78.2
		D4	1279.9	13.8	8025.8	86.2
		D5	1959.5	20.8	7473.5	79.2
		D6	2862.6	32.0	6074.5	68.0
		D7	3387.7	40.7	4938.2	59.3
	2017	D2	2120.3	34.0	4114.1	66.0
		D3	1910.8	27.8	4968.8	72.2
		D4	1427.2	18.3	6363.7	81.7
		D5	1502.7	20.4	5871.6	79.6
		D6	2672.1	39.1	4168.7	60.9
		D7	2891.2	43.3	3792.2	56.7

### 3.4. Differences in Resource Utilization Efficiency

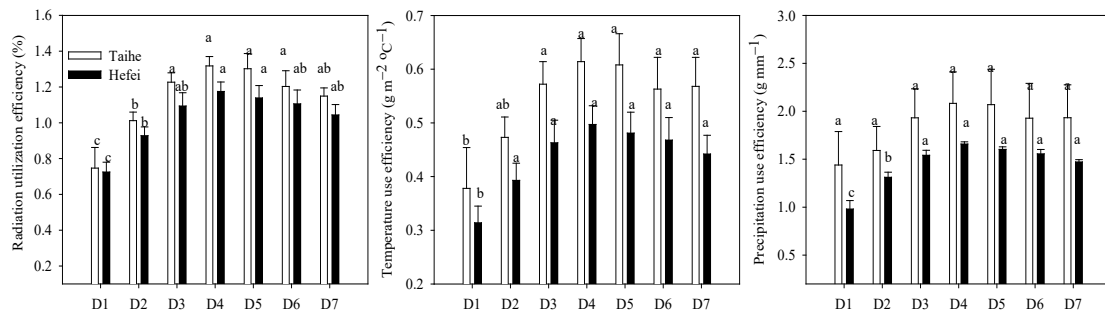
The ranges of solar radiation, AT<sub>10</sub>, and Prec. during the growing season of maize in Taihe and Hefei are shown in Table 7. The range of solar radiation in Taihe was 1441.8~2028.3 MJ m<sup>-2</sup>, with an average of 1792.0 MJ m<sup>-2</sup>, which was 7.8% higher than that of 1340.4~1989.84 MJ m<sup>-2</sup> in Hefei.

Table 7. Climatic resources of different sites.

Climatic Resources	Regions	Ranges
Solar radiation (MJ m <sup>-2</sup> )	Taihe	1441.8~2028.3
	Hefei	1340.4~1989.84
Accumulated temperature ≥ 10 °C (°C)	Taihe	1515.6~1968.6
	Hefei	1715.4~2027.8
Precipitation (mm)	Taihe	358.3~881.1
	Hefei	469.8~1055.2

Differently to solar radiation, AT<sub>10</sub> during the growing season of maize was observed as Taihe < Hefei, with mean values of 1788.4 °C and 1861.9 °C, respectively, and the value in Taihe was 3.9% lower than in Hefei. Similarly, the Prec. showed the same trend as AT<sub>10</sub>. The Prec. values were 582.1 mm and 672.5 mm, respectively, and the value in Taihe was 13.4% lower than in Hefei. In summary, compared to Hefei, Taihe exhibited significantly higher solar radiation but lower AT<sub>10</sub> and Prec. values.

The climatic resource utilization efficiency of different planting densities and regions is shown in Figure 4. In this study, the results showed that D4 and D5 treatments had the highest resource utilization efficiency, and their results were significantly higher than D1 and D2 (Figure 4). We calculated the mean values of RUE, TUE, and PUE from the D3 to D5 treatments in Taihe and Hefei. Taihe had higher RUE, TUE, and PUE values, which were 12.9%, 24.6%, and 26.7% higher than those in Hefei, respectively (Figure 5).



**Figure 4.** Climate resource utilization efficiency of different planting densities in two sites. Note: Different letters above the bars indicate significant differences among the different planting densities of a given site.

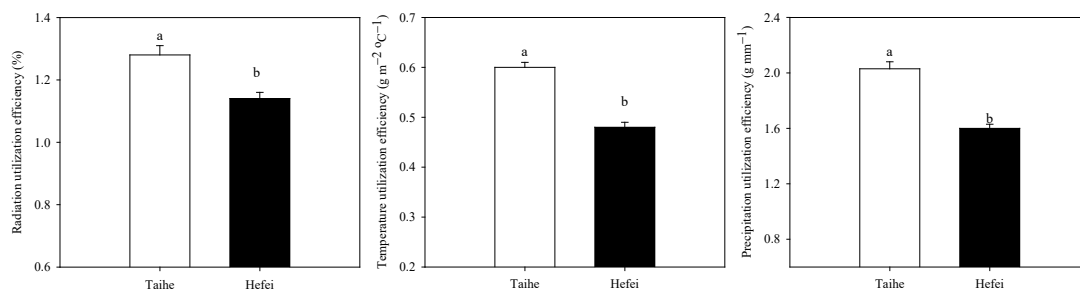


**Figure 5.** Comparison of climate resource utilization efficiencies between Taihe and Hefei. Note: Different letters above the bars indicate significant differences between different sites.

The correlation between solar radiation, AT<sub>10</sub>, precipitation, and grain yield was analyzed. A positive relationship between solar radiation and grain yield ( $R = 0.349, p < 0.01$ ) and a negative relationship with AT<sub>10</sub> ( $R = -0.535, p < 0.01$ ) were found, while there was no significant relationship between precipitation and grain yield ( $R = -0.147, p = 0.217$ ). A stepwise multiple linear regression model was used to analyze solar radiation, AT<sub>10</sub>, and grain yield. The regression equation was  $y = 0.550R - 0.562AT_{10} + 14,593.6$  ( $R = 0.379$ ). In conclusion, the grain yield was positively affected by solar radiation and negatively affected by AT<sub>10</sub>.

### 3.5. Inter-Annual Differences in Yield and Climate

Results showed that solar radiation was positively correlated with yield, while AT<sub>10</sub> was negatively correlated with it. Different sites had different climatic conditions, which also varied in different years. We selected grain yield values at planting densities of  $6 \times 10^4$  plants ha<sup>-1</sup> (D3),  $7.5 \times 10^4$  plants ha<sup>-1</sup> (D4), and  $8 \times 10^4$  plants ha<sup>-1</sup> (D5) and averaged them, then calculated the deviation of the average yield in different years. The deviation rates of yield, solar radiation, and AT<sub>10</sub> in different years and different regions are shown in Figure 6.

The deviation of grain yield in Taihe was from  $-0.8$  to  $26.0\%$ , and it was  $-12.9$  to  $4.0\%$  in Hefei (Figure 6A). In 2015, as solar radiation increased, the grain yield increased in Taihe, which may be because, during the critical period of the flowering stage, there was no occurrence probability of  $T_{max} \geq 35^\circ C$  (Figure 6C). In 2020, the results were the same as in 2015. In these two cases, the grain yield was positively affected by solar radiation, which indicated that with a lower occurrence probability of  $T_{max} \geq 35^\circ C$ , the grain yield increased or decreased as solar radiation increased or decreased. Conversely, in other years with a higher occurrence probability of  $T_{max} \geq 35^\circ C$  ( $28.6\%$  in 2014,  $47.6\%$  in 2017,  $57.1\%$  in 2018, and  $14.3\%$  in 2021), no matter the variation in solar radiation, the grain yield decreased.

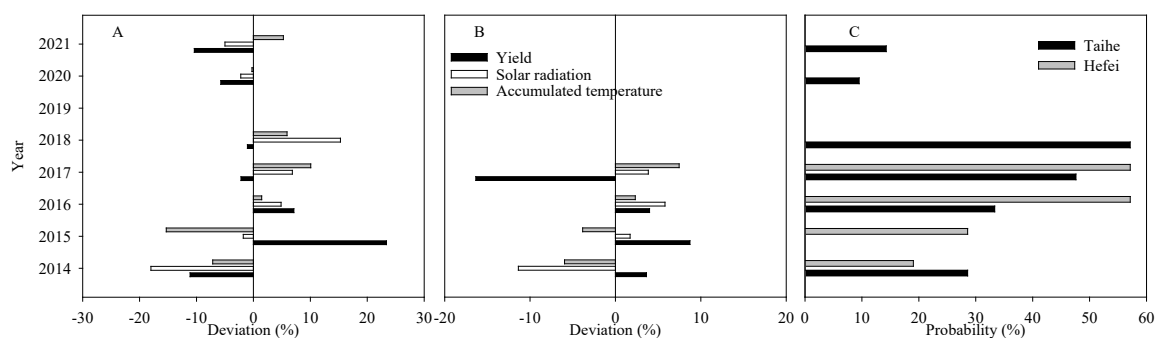


**Figure 6.** Deviation of grain yield, solar radiation, and accumulated temperature  $\geq 10$  °C and the probability of a maximum temperature of  $\geq 35$  °C during the 40 and 60 days after planting in Taihe and Hefei regions. Note: Figure (A) represents the deviation in Taihe, Figure (B) represents the deviation in Hefei, and Figure (C) represents the probability of a maximum temperature of  $\geq 35$  °C.

The average occurrence probability of  $T_{\max} \geq 35$  °C in Hefei was 40.5% (Figure 6C), which was higher than the average value of 27.2% in Taihe. In Hefei, for example, in 2017, the occurrence probability of  $T_{\max} \geq 35$  °C was 69.6% (Figure 6C). The  $T_{\max} \geq 35$  °C lasted for 23 days during the 28- and 60-day durations after planting, and in particular,  $T_{\max} \geq 39$  °C lasted for 7 days, which resulted in a 16.3% decrease in grain yield compared to the other three years.

Overall, the results indicate that regardless of solar radiation being higher or lower, as the rate of  $T_{\max} \geq 35$  °C increased, the grain yield decreased. When the rate of  $T_{\max} \geq 35$  °C was at a lower level, with an increase in solar radiation, the grain yield also increased.

#### 4. Discussion

##### 4.1. Change in Planting Density to Adapt to Climate Change and Improve Yield

In Taihe and Hefei, the solar radiation and accumulated temperature are abundant, and to make full use of climate resources, improving planting density is an effective way to narrow the grain yield gap between actual grain yield and potential grain yield and to increase the grain yield overall [11,36,37]. In this study, the results indicated that as the planting density increased, the grain yield also increased, but when the planting density exceeded the optimal density, the yield decreased, which was consistent with previous research [38]. The optimal planting densities in the two sites were different. The AOPD was  $8.6 \times 10^4$  plants  $\text{ha}^{-1}$  in Taihe, which was higher than that of  $8.0 \times 10^4$  plants  $\text{ha}^{-1}$  in Hefei. However, the AOPDs in these two sites were lower than that in the northwest in China ( $10.5 \times 10^4 \sim 12 \times 10^4$  plants  $\text{ha}^{-1}$ ) and equivalent to that in the southwest ( $8.0 \times 10^4$  plants  $\text{ha}^{-1}$ ), which may be due to the differences in soil properties and climatic conditions [31,38].

The simulated maximum yields in Taihe and Hefei were 10,768.3 kg  $\text{ha}^{-1}$  and 9025.6 kg  $\text{ha}^{-1}$  at the AOPD, respectively, while the actual grain yields were 7115.4 kg  $\text{ha}^{-1}$  and 5654.3 kg  $\text{ha}^{-1}$ , which were calculated from the actual yields in twenty-one counties in SHHH and four counties SE (Figure 7). The actual grain yields achieved 66.1% and 62.6% of the simulated maximum grain yields, which may be owing to the lower actual planting density with the value of  $6 \times 10^4$  plants  $\text{ha}^{-1}$ . Previous studies showed that in the western corn belt of the United States, the average farm yield could achieve over 80% of the simulated potential yield by the Hybrid-Maize Model [39]. However, in China, the average farmer's yield only attained 51% of China's record yield [40], which may be due to the difference in planting density caused by farmer decision-making. Changing farmer attitudes toward the value of optimal planting density could increase farm yields by 12.3% [41]. In this study, the actual density only received 69.7% and 75.9% of the AOPDs; by increasing the actual planting density to the optimal density, the yields could increase by 51.3% and 59.6%. Other research had shown that when the planting density was 19% lower than AOPD, the grain yield would decrease by 39% [38]. Planting density was the most important factor to affect grain yield,

more so than others, such as planting, harvesting date, fertilization, and tillage practice [42]. Changing the planting density within a certain range ( $7.5 \times 10^4 \sim 12 \times 10^4$  plants  $\text{ha}^{-1}$ ) could narrow the grain yield gap [43], which may be because proper planting density establishes an optimum canopy structure [37,44]. An optimum canopy structure, such as a proper leaf area index, can better adapt to solar radiation and accumulated temperature and can result in a higher climatic resource utilization rate [45–47].

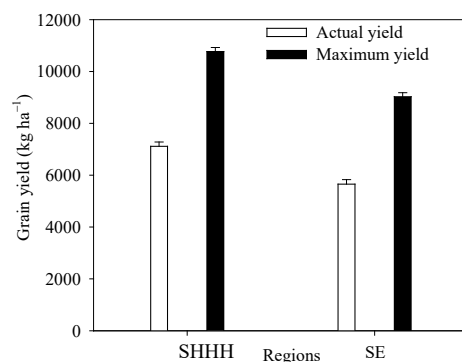


**Figure 7.** The actual yield and stimulated maximum yield in SHHH and SE regions.

Lower planting density induced lower RUE, TUE, and PUE values. Reasonably increasing the planting density was an effective agronomic measure for enhancing the resource utilization efficiency of maize. In this study, D4 and D5 treatments had higher RUE, TUE, and PUE values than other treatments, which was similar to previous findings [48]. When the planting density was in the range of  $6.9 \sim 8.6 \times 10^4$  plants  $\text{ha}^{-1}$ , the maize population could make full use of the climatic resources, resulting in a higher grain yield, and this result is consistent with the simulated results. A lower planting density results in a lower LAI, which cannot match or take advantage of the abundant solar radiation and temperature resources, causing a waste of solar radiation [1] and a decrease in DMA. In this study, lower planting density produced lower DMA, especially DMA at the post-silking stage. Moreover, when the planting density was too large, the LAI became too high, causing self-shading [45], and the DMT before the silking stage was higher than optimal planting density, the contribution of dry matter at the post-silking stage to the grain weight was higher, which resulted in yield loss. Optimal planting density could promote rapid canopy closure and improve the potential capacity of the crop canopy to capture climatic resources [49]. Sub-optimal and up-optimal densities had a negative impact on the efficiency with which the crop or plant converts intercepted radiation into grain sink capacity [50]. In this study, D4 and D5 treatments had higher DMA at the post-silking stage and higher CDMGW. Overall, in the Taihe and Hefei sites, a proper increase in planting density could be an effective way to increase the grain yield and narrow the grain gap via a higher climatic resource utilization efficiency.

#### 4.2. Heat Resource Has a Negative Effect on the Grain Yield

The yields sometimes varied among different ecological areas with the same planting density [31]. Many studies reported that climatic conditions and cultivation management measures affected yield and its components differently between different regions [51]. In this study, Taihe produced a significantly higher grain yield than Hefei by 9.7–23.6%, which may be induced by the difference in kernel number per ear. Previous studies reported that kernel number accounted for most of the variation in grain yield [52,53], and kernel number was the main numerical component contributing to grain yield variations across densities [54], which was similar to our result.

In this study, the RUE, TUE, and PUE values in Taihe were significantly higher than those in Hefei. Regression analysis showed that grain yield was not limited by precipitation due to the ample amount of precipitation, which was different from the Northern Huang-Huai-Hai Plain of China and other ecological areas in the world [48,55], while  $AT_{10}$  had

a negative effect on the grain yield, and was the main factor affecting the grain yield, compared to the solar radiation. It has been reported that the total radiation and thermal time during the growth period would positively affect the grain yield in the northern maize area, and regional radiation was the main factor affecting maize production compared to the thermal time [23], which was different from our finding. The difference may be owing to the higher occurrence rate of  $T_{\max} \geq 35$  °C. In the Taihe and Hefei regions, the climatic conditions were different from those in northern China. Maximum temperatures exceeding 35 °C often occurred, and the occurrence probabilities 40~60 days after planting were about 27.2% in Taihe and 40.5% in Hefei, which may result in a high-temperature disaster risk during the flowering of summer maize. The impact of high temperature on yield relates to the timing of the occurrence [3]. During the flowering stage, high temperatures induce death of the flower and failure in pollination, and pollen viability determines kernel number [56], which may be the reason for the difference in kernel numbers per ear between the two sites, resulting in a reduction in grain yield. The WOFOST model predicted that under climate conditions in the future, the decrease in yield might be partially alleviated by changes in phenology and sowing dates [57]. In Ethiopia, researchers formulated that under such climate conditions, changes in hybrid variety and nitrogen fertilization management may improve grain yield [58]. In the future, heat waves will become more frequent, longer, and more intense [2]. Previous studies revealed that the annual mean temperature increase in the Huang-Huai-Hai region during 1979–2014 was 0.37 °C per 10 a, and the probability of concurrent drought and heat events increased from the northeast to the southwest in the Huang-Huai-Hai region, which mainly occurred during the vegetative period [2,59]. Extreme heat during the silking stage decreases the photosynthetic capacity, shortens grain-filling duration, and decreases grain-filling rates. When high temperature coincides with tasseling and early grain filling stage, yield decreases dramatically, and farmers can hardly alleviate this situation [2]. Overall, regardless of higher solar radiation or lower radiation, as the rate of maximum temperature exceeding 35 °C increased, grain yield decreased. When the rate of maximum temperature exceeding 35 °C decreased, with an increase in solar radiation, the grain yield increased.

Improving climatic resource utilization efficiency and increasing local grain yield are still the main objectives in China. In this study, we formulated the agronomic measurements to increase grain yield and clarified the main limiting climatic factors. Due to global climate change, severe weather events will occur more frequently. In order to adapt to local climatic factors and maximize the utilization efficiency of climatic resources, it is necessary to formulate cultivation measurements with regional characteristics. In Taihe, which belongs to SHHH, measures to increase the planting density can be used to increase production, while in Hefei, which belongs to SE, due to the lower planting density and kernel number per ear compared to SHHH, the measures of increasing planting density and planting large-ear maize hybrid varieties may be used to improve yield. Similarly, the demand for new crop varieties with excellent comprehensive traits is even more urgent due to global warming. High-temperature tolerance of maize varieties should be used as an important breeding index in these two regions. However, our experimental sites were not sufficient. In the future, we will arrange more experimental sites on a larger scale to more accurately guide local corn production.

## 5. Conclusions

This study determined the AOPD in Taihe and Hefei sites and increased the planting density from  $6.0 \times 10^4$  plants  $\text{ha}^{-1}$  to  $8.6 \times 10^4$  plants  $\text{ha}^{-1}$  in Taihe and  $7.9 \times 10^4$  plants  $\text{ha}^{-1}$  in Hefei, which could enhance the grain yield by 51.3% and 59.6%, respectively. D4 and D5 treatments had higher RUE, TUE, and PUE values than the other treatments. As for the different sites, the RUE, TUE, and PUE values in Taihe were 12.9%, 24.6%, and 26.7% higher than those of Hefei. Solar radiation had a positive effect on the grain yield, while  $AT_{10}$  had a negative effect on the grain yield. Compared to solar radiation  $AT_{10}$  was the main climatic factor affecting the grain yield, which may be due to the high

occurrence probability of  $T_{\max} \geq 35$  °C. Ultimately, in order to adapt to local climatic factors and maximize the utilization efficiency of climatic resources, it is necessary to formulate cultivation measurements with regional characteristics. In the future, increasing planting density and alleviating heat stress may enhance grain yield.

**Author Contributions:** Conceptualization, S.W. and W.W.; methodology, W.W., L.Z. and C.P.; software, W.W., W.Y., Y.X. and Z.C.; validation, W.M., W.W. and Z.C.; formal analysis, W.W. and X.C.; investigation, W.W., C.P. and L.J.; resources, W.Y. and L.J.; data curation, W.W.; writing—original draft preparation, W.W., S.W. and W.M.; writing—review and editing, W.W., S.W. and W.M.; visualization, W.W.; supervision, S.W.; project administration, S.W.; funding acquisition, W.W. and L.Z. All authors have read and agreed to the published version of the manuscript.

**Funding:** This research was funded by the Talent Project of the Anhui Academy of Agricultural Sciences (QNYC-202116), the Key Research and Development Program of Anhui Province (202204c06020007), and the National Key Research and Development Program of China (2017YFD0301307).

**Data Availability Statement:** Data available from the corresponding author.

**Acknowledgments:** The authors thank the anonymous reviewers for their valuable comments and suggestions. The first author thanks all the other author's support and assistance.

**Conflicts of Interest:** The authors declare no conflict of interest.

## Abbreviations

SHHH	Southern Huang-Huai-Hai maize region
SE	Hilly maize area in the southeast
AOPD	Agronomic optimal planting density
$T_{mean}$	The mean temperature
$T_{max}$	The maximum temperature
Prec.	Precipitation
AT <sub>10</sub>	Accumulated temperature $\geq 10$ °C
RUE	Solar radiation utilization efficiency
TUE	Temperature utilization efficiency
PUE	Precipitation utilization efficiency
DMA	Dry matter accumulation
DMT	Dry matter translocation
CDMGW	The contribution of dry matter at the post-silking stage to the grain weight

## References

- Li, R.F.; Zhang, G.Q.; Liu, G.Z.; Wang, K.; Xie, R.Z.; Hou, P.; Ming, B.; Wang, Z.G.; Li, S.K. Improving the yield potential in maize by constructing the ideal plant type and optimizing the maize canopy structure. *Food Energy Secur.* **2021**, *10*, e312. [[CrossRef](#)]
- Wang, L.J.; Liao, S.H.; Huang, S.B.; Ming, B.; Meng, Q.F.; Wang, P. Increasing concurrent drought and heat during the summer maize season in Huang-Huai-Hai Plain, China. *Int. J. Climatol.* **2018**, *38*, 3177–3190. [[CrossRef](#)]
- Edreira, J.I.R.; Otegui, M.E. Heat stress in temperate and tropical maize hybrids: A novel approach for assessing sources of kernel loss in field conditions. *Field Crops Res.* **2013**, *142*, 58–67. [[CrossRef](#)]
- Ma, D.L.; Xie, R.Z.; Zhang, F.L.; Li, J.; Li, S.M.; Long, H.L.; Liu, Y.; Guo, Y.Q.; Li, S.K. Genetic contribution to maize yield gain among different locations in China. *Maydica* **2015**, *60*, 1–8.
- Feng, Y.; Cui, X.; Shan, H.; Shi, Z.S.; Li, F.H.; Wang, H.W.; Zhu, M.; Zhong, X.M. Effects of solar radiation on photosynthetic physiology of barren stalk differentiation in maize. *Plant Sci.* **2021**, *312*, 111046. [[CrossRef](#)]
- Yang, Y.S.; Guo, X.X.; Hou, P.; Xue, J.; Liu, G.Z.; Liu, W.M.; Wang, Y.H.; Zhao, R.L.; Ming, B.; Xie, R.Z.; et al. Quantitative effects of solar radiation on maize lodging resistance mechanical properties. *Field Crops Res.* **2020**, *255*, 107906. [[CrossRef](#)]
- Zhang, M.; Chen, T.; Hojatollah, L.; Feng, X.M.; Cao, T.H.; Qian, C.R.; Deng, A.X.; Song, Z.W.; Zhang, W.J. How plant density affects maize spike differentiation, kernel set, and grain yield formation in Northeast China? *J. Integr. Agric.* **2018**, *17*, 1745–1757. [[CrossRef](#)]
- Xue, H.Y.; Han, Y.C.; Li, Y.B.; Wang, G.P.; Lu, F.; Fan, Z.Y.; Du, W.L.; Yang, B.F.; Mao, S.C. Spatial distribution of light interception by different plant population densities and its relationship with yield. *Field Crops Res.* **2015**, *184*, 17–27. [[CrossRef](#)]
- Yang, J.S.; Gao, H.Y.; Peng, L.; Geng, L.I.; Dong, S.T.; Zhang, J.W. Effects of planting density and row spacing on canopy apparent photosynthesis of high-yield summer corn. *Acta Agron. Sin.* **2010**, *36*, 1226–1235. [[CrossRef](#)]

10. Gonzalez, V.H.; Tollenaar, M.; Bowman, A.; Good, B.; Lee, E.A. Maize yield potential and density tolerance. *Crop Sci.* **2018**, *58*, 472–485. [[CrossRef](#)]
11. Liu, G.Z.; Yang, H.S.; Xie, R.Z.; Yang, Y.S.; Liu, W.M.; Guo, X.X.; Xue, J.; Ming, B.; Wang, K.R.; Hou, P.; et al. Genetic gains in maize yield and related traits for high-yielding cultivars released during 1980s to 2010s in China. *Field Crops Res.* **2021**, *270*, 108223. [[CrossRef](#)]
12. Aschonitis, V.G.; Mastrocicco, M.; Colombani, N.; Salemi, E.; Kazakis, N.; Voudouris, K.; Castaldelli, G. Assessment of the intrinsic vulnerability of agricultural land to water and nitrogen losses via deterministic approach and regression analysis. *Water Air Soil Pollut.* **2012**, *223*, 1605–1614. [[CrossRef](#)]
13. Assefa, Y.; Carter, P.; Hinds, M.; Bhalla, G.; Schon, R.; Jeschke, M.; Paszkiewicz, S.; Smith, S.; Ciampitti, I.A. Analysis of long term study indicates both agronomic optimal plant density and increase maize yield per plant contributed to yield gain. *Sci. Rep.* **2018**, *8*, 4937. [[CrossRef](#)]
14. Sangoi, L. Understanding plant density effects on maize growth and development: An important issue to maximize grain yield. *Ciência Rural* **2000**, *31*, 159–168. [[CrossRef](#)]
15. Chen, G.Z.; Wu, P.; Wang, J.Y.; Zhou, Y.D.; Ren, L.Q.; Cai, T.; Zhang, P.; Jia, Z.K. How do different fertilization depths affect the growth, yield, and nitrogen use efficiency in rain-fed summer maize? *Field Crops Res.* **2023**, *290*, 108759. [[CrossRef](#)]
16. Zhao, J.; Yang, X.G.; Liu, Z.J.; Lv, S.; Wang, J.; Dai, S.W. Variations in the potential climatic suitability distribution patterns and grain yields for spring maize in Northeast China under climate change. *Clim. Chang.* **2016**, *137*, 29–42. [[CrossRef](#)]
17. Begna, S.H.; Hamilton, R.L.; Dwver, L.M.; Stewart, D.W.; Smith, D.L. Effects of population density and planting pattern on the yield and yield components of leafy reduced-stature maize in a short-season area. *J. Agron. Crop Sci.* **1997**, *179*, 9–17. [[CrossRef](#)]
18. Tokatlidis, I.S.; Has, V.; Melidis, V.; Has, I.; Mylonas, I.; Evgenidis, G.; Copandean, A.; Ninou, E.; Fasoula, V.A. Maize hybrids less dependent on high plant densities improve resource-use efficiency in rainfed and irrigated conditions. *Field Crops Res.* **2011**, *120*, 345–351. [[CrossRef](#)]
19. Jia, Q.M.; Sun, L.F.; Mou, H.Y.; Ali, S.; Liu, D.H.; Zhang, Y.; Zhang, P.; Ren, X.L.; Jia, Z.K. Effects of planting patterns and sowing densities on grain-filling, radiation use efficiency and yield of maize (*Zea mays* L.) in semi-arid Regions. *Agric. Water Manag.* **2017**, *201*, 287–298. [[CrossRef](#)]
20. Wang, T.X.; Li, N.; Li, Y.; Lin, H.X.; Yao, N.; Chen, X.G.; Liu, D.L.; Yu, Q.; Feng, H. Impact of climate variability on grain yields of spring and summer maize. *Comput. Electron. Agric.* **2022**, *199*, 107101. [[CrossRef](#)]
21. Yu, Y.; Jiang, Z.H.; Wang, G.J.; Kattel, G.R.; Chuai, X.W.; Shang, Y.; Zou, Y.F.; Miao, L.J. Disintegrating the impact of climate change on maize yield from human management practices in China. *Agric. For. Meteorol.* **2022**, *327*, 109235. [[CrossRef](#)]
22. Wang, J.; Wang, E.; Yin, H.; Feng, L.P.; Zhao, Y.X. Differences between observed and calculated solar radiations and their impact on simulated crop yields. *Field Crops Res.* **2015**, *176*, 1–10. [[CrossRef](#)]
23. He, H.Y.; Hu, Q.; Li, R.; Pan, X.B.; Huang, B.X.; He, Q.J. Regional gap in maize production, climate and resource utilization in China. *Field Crops Res.* **2020**, *254*, 107830. [[CrossRef](#)]
24. Liu, Y.E.; Hou, P.; Xie, R.Z.; Hao, W.P.; Li, S.K.; Mei, X.R. Spatial variation and improving measures of the utilization efficiency of accumulated temperature. *Crop Sci.* **2015**, *55*, 1806–1817. [[CrossRef](#)]
25. Yang, Y.W.; Yu, Q.; Wang, J. Spatio-temporal variations of principal climatic factors in north china and part of East China within past 40 years. *Resour. Sci.* **2004**, *26*, 45–50.
26. Zhang, L.L.; Zhang, Z.; Luo, Y.C.; Cao, J.; Li, Z.Y. Optimizing genotype-environment-management interactions for maize farmers to adapt to climate change in different agro-ecological zones across China. *Sci. Total Environ.* **2020**, *728*, 138614. [[CrossRef](#)]
27. Zhang, Z.T.; Yang, X.G.; Liu, Z.J.; Bai, F.; Sun, S.; Nie, J.Y.; Gao, J.Q.; Ming, B.; Xie, R.Z.; Li, S.K. Spatio-temporal characteristics of agro-climatic indices and extreme weather events during the growing season for summer maize (*Zea mays* L.) in Huanghuaihai region, China. *Int. J. Biometeorol.* **2020**, *64*, 827–839. [[CrossRef](#)]
28. Hou, P.; Liu, Y.; Liu, W.M.; Yang, H.S.; Xie, R.Z.; Wang, K.R.; Ming, B.; Liu, G.Z.; Xue, J.; Wang, Y.H.; et al. Quantifying maize grain yield losses caused by climate change based on extensive field data across China. *Resour. Conserv. Recycl.* **2021**, *174*, 105811. [[CrossRef](#)]
29. Xiao, D.P.; Liu, D.L.; Wang, B.; Feng, P.Y.; Waters, C. Designing high-yielding maize ideotypes to adapt changing climate in the North China Plain. *Agric. Syst.* **2020**, *181*, 102805. [[CrossRef](#)]
30. Liu, Y.; Wang, E.L.; Yang, X.G.; Wang, J. Contributions of climatic and crop varietal changes to crop production in the North China Plain, since 1980s. *Glob. Chang. Biol.* **2010**, *16*, 2287–2299. [[CrossRef](#)]
31. Xu, W.J.; Liu, C.W.; Wang, K.R.; Xie, R.Z.; Ming, B.; Wang, Y.H.; Zhang, G.Q.; Liu, G.Z.; Zhao, R.L.; Fan, P.P.; et al. Adjusting maize plant density to different climatic conditions across a large longitudinal distance in China. *Field Crops Res.* **2017**, *212*, 126–134. [[CrossRef](#)]
32. Gao, Y.K.; Zhao, H.F.; Zhao, C.; Hu, G.H.; Zhang, H.; Liu, X.; Li, N.; Hou, H.Y.; Li, X. Spatial and temporal variations of maize and wheat yield gaps and their relationships with climate in China. *Agric. Water Manag.* **2022**, *270*, 107714. [[CrossRef](#)]
33. Wu, W.M.; Wang, S.J.; Chen, H.J.; Song, Y.H.; Zhang, L.; Chen, P.; Jing, L.L.; Li, J.C. Optimal nitrogen regimes compensate for the impacts of seedling subjected to waterlogging stress in summer maize. *PLoS ONE* **2018**, *13*, e0206210. [[CrossRef](#)]
34. Wu, W.M.; Wang, S.J.; Zhang, L.; Li, J.C.; Song, Y.H.; Peng, C.; Chen, X.; Jing, L.L.; Chen, H.J. Subsoiling improves the photosynthetic characteristics of leaves and water use efficiency of rainfed summer maize in the southern Huang-Huai-Hai plain of China. *Agronomy* **2020**, *10*, 465. [[CrossRef](#)]

35. Chang, Q. Spati-Temporal Variation of the Yield in Wheat-Maize Production System and the Distribution Differences of Radiation and Heat Use Efficiency in Henan Province. Master's Thesis, China Agricultural University, Beijing, China, 2016.
36. Liu, G.; Liu, W.; Hou, P.; Ming, B.; Yang, Y.; Guo, X.; Xie, R.; Wang, K.; Li, S. Reducing maize yield gap by matching plant density and solar radiation. *J. Integr. Agric.* **2020**, *19*, 2–9. [[CrossRef](#)]
37. Ren, B.Z.; Liu, W.; Zhang, J.W.; Dong, S.T.; Liu, P.; Zhao, B. Effects of plant density on the photosynthetic and chloroplast characteristics of maize under high-yielding conditions. *Sci. Nat.* **2017**, *104*, 12. [[CrossRef](#)]
38. Luo, N.; Wang, X.Y.; Hou, J.M.; Wang, Y.Y.; Wang, P.; Meng, Q.F. Agronomic optimal plant density for yield improvement in the major maize regions of China. *Crop Sci.* **2020**, *60*, 1580–1590. [[CrossRef](#)]
39. Grassini, P.; Thorburn, J.; Burr, C.; Cassman, K.G. High-yield irrigated maize in the Western U.S. Corn Belt: I. On-farm yield, yield potential, and impact of agronomic practices. *Field Crops Res.* **2011**, *120*, 142–150. [[CrossRef](#)]
40. Meng, Q.F.; Hou, P.; Wu, L.; Chen, X.P.; Cui, Z.L.; Zhang, F.S. Understanding production potentials and yield gaps in intensive maize production in China. *Field Crops Res.* **2013**, *143*, 91–97. [[CrossRef](#)]
41. An, Z.C.; Wang, C.; Jiao, X.Q.; Kong, Z.L.; Jiang, W.; Zhang, D.; Ma, W.Q.; Zhang, F.S. Methodology of analyzing maize density loss in smallholder's fields and potential optimize approach. *Agriculture* **2021**, *11*, 480. [[CrossRef](#)]
42. Zhang, W.F.; Cao, G.X.; Li, X.L.; Zhang, H.Y.; Wang, C.; Liu, Q.Q.; Chen, X.P.; Cui, Z.L.; Shen, J.B.; Jiang, R.F.; et al. Closing yield gaps in China by empowering smallholder farmers. *Nature* **2016**, *537*, 622–671. [[CrossRef](#)] [[PubMed](#)]
43. Sun, H.Y.; Zhang, X.Y.; Wang, E.L.; Chen, S.Y.; Shao, L.W.; Qin, W.L. Assessing the contribution of weather and management to the annual yield variation of summer maize using APSIM in the North China Plain. *Field Crops Res.* **2016**, *194*, 94–102. [[CrossRef](#)]
44. Deng, J.M.; Ran, J.Z.; Wang, Z.Q.; Fan, Z.X.; Wang, G.X.; Ji, M.F.; Liu, J.; Wang, Y.; Liu, J.Q.; Brown, J.H. Models and tests of optimal density and maximal yield for crop plants. *Proc. Natl. Acad. Sci. USA* **2012**, *109*, 15823–15828. [[CrossRef](#)]
45. Srinivasan, V.; Kumar, P.; Long, S.P. Decreasing, not increasing, leaf area will raise crop yields under global atmospheric change. *Glob. Change Biol.* **2017**, *23*, 1626–1635. [[CrossRef](#)]
46. Robles, M.; Ciampitti, I.A.; Vyn, T.J. Responses of maize hybrids to twin-row spatial arrangement at multiple plant densities. *Agron. J.* **2012**, *104*, 1747–1756. [[CrossRef](#)]
47. Zhao, J.F.; Guo, J.P.; Mu, J. Exploring the relationships between climatic variables and climate-induced yield of spring maize in Northeast China. *Agric. Ecosyst. Environ.* **2015**, *207*, 79–90. [[CrossRef](#)]
48. Zhai, L.C.; Zhang, L.H.; Yao, H.P.; Zheng, M.J.; Ming, B.; Xie, R.Z.; Zhang, J.T.; Jia, X.L.; Ji, J.J. The optimal cultivar × sowing date × plant density for grain yield and resource use efficiency of summer maize in the Northern Huang-Huai-Hai Plain of China. *Agriculture* **2022**, *12*, 7. [[CrossRef](#)]
49. Bu, L.D.; Chen, X.P.; Li, S.Q.; Liu, J.L.; Zhu, L.; Luo, S.S.; Hill, R.L.; Zhao, Y. The effect of adapting cultivars on the water use efficiency of dryland maize (*Zea mays* L.) in northwestern China. *Agric. Water Manag.* **2015**, *148*, 1–9. [[CrossRef](#)]
50. Andrade, F.H.; Uhart, S.A.; Frugone, M.I. Intercepted radiation at flowering and kernel number in maize: Shade versus plant density effects. *Crop Sci.* **1983**, *33*, 482–485. [[CrossRef](#)]
51. Wang, J.; Wang, E.; Yin, H.; Feng, L.; Zhang, J. Declining yield potential and shrinking yield gaps of maize in the North China Plain. *Agric. For. Meteorol.* **2014**, *195*, 89–101. [[CrossRef](#)]
52. Fischer, K.S.; Palmer, A.F. Tropical Maize. In *The Physiology of Tropical Field Crops*; Goldsworthy, P.R., Fischer, N., Eds.; Wiley: New York, NY, USA, 1984; pp. 213–248.
53. Otegui, M.E. Prolificacy and grain yield components in modern Argentinian maize hybrids. *Maydica* **1995**, *40*, 371–376.
54. Cerrudo, D.; Hernández, M.; Tollenaar, M.; Vega, C.R.C.; Echarte, L. Kernel number response to plant density in tropical, temperate, and tropical × temperate maize hybrids. *Crop Sci.* **2020**, *260*, 381–390. [[CrossRef](#)]
55. Umesh, B.; Reddy, K.S.; Polisgowdar, B.S.; Maruthi, V.; Satishkumar, U.; Ayyanagoudar, M.S.; Rao, S.; Veeresh, H. Assessment of climate change impact on maize (*Zea mays* L.) through aquacrop model in semi-arid alfisol of southern Telangana. *Agric. Water Manag.* **2022**, *274*, 107950. [[CrossRef](#)]
56. Lizaso, J.I.; Ruiz-Ramos, M.; Rodríguez, L.; Gabaldon-Lealb, C.; Oliveirac, J.A.; Loriteb, I.J.; Sánchez, D.; García, E.; Rodríguez, A. Impact of high temperatures in maize: Phenology and yield components. *Field Crops Res.* **2018**, *216*, 129–140. [[CrossRef](#)]
57. Bassu, S.; Fumagalli, D.; Toreti, A.; Ceglar, A.; Giunta, F.; Motzo, R.; Zajac, Z.; Niemeyer, S. Modelling potential maize yield with climate and crop conditions around flowering. *Field Crops Res.* **2021**, *271*, 108226. [[CrossRef](#)]
58. Chekole, F.C.; Ahmed, A.M. Future climate implication on maize (*Zea mays*) productivity with adaptive options at Harbu district, Ethiopia. *J. Agric. Food Res.* **2023**, *11*, 100480. [[CrossRef](#)]
59. Wang, H.T.; Zhang, C.H.; Fang, Y.; Chu, J.H.; Yan, Z.; Zhou, G.X.; Wang, L.; Yang, W.; Shen, G.L.; Wang, H. The impact of climate change on crop breeding strategies in China. *Chin. Agric. Sci. Bull.* **2022**, *38*, 64–74.

**Disclaimer/Publisher's Note:** The statements, opinions and data contained in all publications are solely those of the individual author(s) and contributor(s) and not of MDPI and/or the editor(s). MDPI and/or the editor(s) disclaim responsibility for any injury to people or property resulting from any ideas, methods, instructions or products referred to in the content.